On the necessity of symmetric positional coupling for string stability

Dan Martinec, Ivo Herman, and Michael Šebek

***Abstract*—We consider a distributed system with identical agents and asymmetric bidirectional control, where the asymmetry is due to different controllers, which we describe by transfer functions. By applying the wave transfer function approach, it is shown that, if there are two integrators in the dynamics of agents, then the positional coupling must be symmetric, otherwise the system is string unstable. This finding holds also for a distributed system with complex interaction topology due to the local nature of the wave transfer function. The main advantage of the transfer function approach is that it allows to analyse bidirectional control with arbitrary complexity of asymmetry in the controllers, for instance, the control with symmetric positional but asymmetric velocity couplings.**

***Index Terms*—Asymmetric control, string stability, distributed system, travelling waves, wave transfer function**

I. Introduction

Although each agent in a distributed system is usually well designed and asymptotically stable, the interaction between agents can trigger undesirable phenomena such as string instability. There are several definitions of the string instability, see [1], [2] or [3]. They all describe how the disturbance acting on agent amplifies as it propagates in the system. Similar analytical measures of system performance are harmonic stability [4], flock stability [5] and coherence [6].

One of the most studied distributed system is a vehicular platoon, where the interaction topology is a path graph. Each agent of such a system, except for the first and last, measures the distance, i.e. its relative position, to the nearest neighbours. For such a case, we require two integrators to be present in the open-loop model of each agent so that the agent can track the leader travelling with a constant velocity with the zero steady-state error.

It was shown in [7] that the string instability is unavoidable for the agents with two integrators under an unidirectional interaction, therefore, an asymmetric bidirectional scheme was introduced. Later, it was shown in [8] that the same asymmetry for all states used for coupling causes a nonzero lower bound on the distributed-system eigenvalues, which guarantees the controllability of a system with even a large number of agents, see [9]. The disadvantage of such an asymmetric bidirectional control of agents with two integrators, as shown in [4] and [10], is that the system is harmonically unstable, meaning that the $\mathcal{H}_\infty$ norm of transfer functions between the agents scales exponentially with the number of agents in the system.

Recently, papers [11] and [5] introduce a novel type of asymmetric bidirectional control by assuming nonequal asymmetries between the output states. They showed that different couplings between the positions and velocities in the double integrator system can be beneficial for decreasing the transient and overshoots in the system response. The latter paper also suggests that the symmetry in the positional coupling is necessary for the asymptotic and flock stabilities of an oscillator array. The reasoning of both papers were based on mathematical simulations and reasonable conjectures, which raise the following questions. Can the 'symmetry' condition be generalized for more complex agent dynamics? Is the symmetric coupling necessary for other types of graphs than a path graph? Answering these questions is the main aim of this paper.

We adopt the wave approach from [12] and generalize it for a homogenous-asymmetric path graph, which represents a distributed system where all the agents are identical but the coupling between them is asymmetric. Unlike the traditional Laplacian approach, e.g. [13], the wave approach allows us to describe how the information is locally propagated from an agent to its immediate neighbours. By analyzing this local behaviour, we can study the performance of a distributed system, for instance, the string (in)stability. Moreover, the wave approach allows the treatment of arbitrary asymmetry in the controllers, for instance, different positional and velocity couplings. We show that symmetric coupling between the agent's positions, represented by the identical DC gains of the controllers, is necessary for the string stability. This result holds for arbitrary graph and agent's model, which is a complementary result to prior findings about the string stability of asymmetric bidirectional control.

The paper is organized as follows. Section II introduces model of agent in a distributed system. Section III derives properties of the wave propagation in a distributed system with path graph topology that are necessary to state the main result in Theorem 3 in Section IV. The numerical validation of the proposed approach is given Section V. Section VI shows that the result in Theorem 3 holds even for distributed system with complex interaction topology.

II. Mathematical preliminaries

We consider a formation of identical agents with a path graph interaction topology, for instance, a platoon of vehicles on a highway. The goal of the formation is to drive along a line with equal distances between the agents.

All authors are with the Faculty of Electrical Engineering, Czech Technical University in Prague, Department of Control Engineering, Karlovo namesti 13, 121 35 Prague, Czech Republic. E-mail address: {martinec.dan, ivo.herman, sebekm1}@fel.cvut.cz

The research was supported by the Grant Agency of the Czech Republic within the projects GACR 13-06894S (I. H.).

The dynamics of agents is described by a linear single-input-single-output model, the transfer function $P(s)$. The output is the position of the agent, $X_n(s)$, described as

$$X_n(s) = P(s)U_n(s), \tag{1}$$

where n denotes index of the agent and $U_n(s)$ is the input to the agent generated by the local controllers onboard the agent. The goal of the controllers is to equalize relative distances to the immediate neighbours. Each agent has two controllers $C_\mathrm{f}(s)$ and $C_\mathrm{r}(s)$ that control the front and rear distance of the agent, respectively. We describe the controllers by transfer functions, which allows the representation of arbitrary couplings between the agents. In other words, the controllers may be of an arbitrary order and structure. We consider that each agent has the same set of controllers but the two controllers may be different, i.e. $C_\mathrm{f}(s) \neq C_\mathrm{r}(s)$. Then

$$\begin{aligned} U_n(s) =& C_\mathrm{f}(s)\left(X_{n-1}(s) - X_n(s)\right) \\ &+ C_\mathrm{r}(s)(X_{n+1}(s) - X_n(s)). \end{aligned} \tag{2}$$

The resulting model of the nth agent is shown in Fig. 1 and described as

$$\begin{aligned} X_n(s) =& M_\mathrm{f}(s)(X_{n-1}(s) - X_n(s)) \\ &+ M_\mathrm{r}(s)(X_{n+1}(s) - X_n(s)), \end{aligned} \tag{3}$$

where $M_\mathrm{f}(s) = C_\mathrm{f}(s)P(s)$ and $M_\mathrm{r}(s) = C_\mathrm{r}(s)P(s)$. We allow the controllers to be arbitrary but assume that $M_\mathrm{f}(s)$ and $M_\mathrm{r}(s)$ have the same number of integrators.

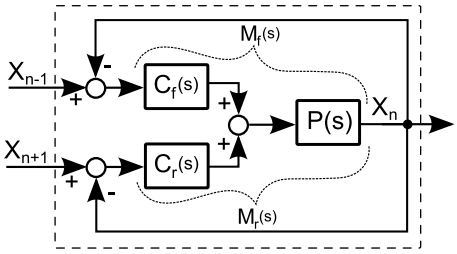

Fig. 1: The model of nth agent.

The first agent ($n = 0$), the so-called leader, is externally controlled and serves as a reference signal for the distributed system. The rear-end agent ($n = N$) of the path graph is described as

$$X_N(s) = M_\mathrm{f}(s)(X_{N-1}(s) - X_N(s)). \tag{4}$$

It is convenient to express $M_\mathrm{f}(s)$ and $M_\mathrm{r}(s)$ as

$$M_\mathrm{f}(s) = \frac{1}{s^p}\frac{n_\mathrm{f}(s)}{d_\mathrm{f}(s)} = \frac{1}{s^p}\frac{\sum_{k=0}^{L_\mathrm{f}} n_{\mathrm{f},k}s^k}{\sum_{k=0}^{K_\mathrm{f}} d_{\mathrm{f},k}s^k}, \tag{5}$$

$$M_\mathrm{r}(s) = \frac{1}{s^p}\frac{n_\mathrm{r}(s)}{d_\mathrm{r}(s)} = \frac{1}{s^p}\frac{\sum_{k=0}^{L_\mathrm{r}} n_{\mathrm{r},k}s^k}{\sum_{k=0}^{K_\mathrm{r}} d_{\mathrm{r},k}s^k}, \tag{6}$$

where p is the number of integrators, which is the same for both transfer functions, K_f, L_f, K_r and L_r is the order of polynomial $n_\mathrm{f}(s)$, $d_\mathrm{f}(s)$, $n_\mathrm{r}(s)$ and $d_\mathrm{r}(s)$, respectively, and $n_{\mathrm{f},k}$, $d_{\mathrm{f},k}$, $n_{\mathrm{r},k}$ and $d_{\mathrm{r},k}$ are their coefficients. Without lost of generality we assume $n_{\mathrm{f},0} \neq 0$, $n_{\mathrm{r},0} \neq 0$ and $d_{\mathrm{f},0} = d_{\mathrm{r},0} = 1$.

The traditional asymmetric bidirectional control, see [9] or [4], assumes that $M_\mathrm{f}(s) = \mu M_\mathrm{r}(s)$, where μ is a constant gain. We allow the asymmetry to be more general than scaling and focus on the relation between the kth coefficients of (5) and (6).

Definition 1. We say that the distributed system has *symmetric positional coupling* if the open-loop model of an agent has

$$\frac{n_{\mathrm{f},0}}{d_{\mathrm{f},0}} = \frac{n_{\mathrm{r},0}}{d_{\mathrm{r},0}}. \tag{7}$$

In other words, the positional coupling is symmetric if the DC gain of $M_\mathrm{f}(s)/M_\mathrm{r}(s)$ is equal to one. Similarly, the velocity coupling is symmetric if $n_{\mathrm{f},1}/d_{\mathrm{f},1} = n_{\mathrm{r},1}/d_{\mathrm{r},1}$.

III. Wave Transfer Function for Asymmetric Bidirectional Connection

The bidirectional property of locally controlled agents causes that any change in the position of the leader is propagated through the distributed system as a *wave*. When the wave reaches the rear-end agent, it reflects and propagates back to the leader, where it reflects again. This section describes the propagation of this wave.

The basic idea is to describe the position of the nth agent in a distributed system with a path graph topology by two components, $A_n(s)$ and $B_n(s)$, that represent two waves propagating along a distributed system in the forward and backward directions, respectively. The mathematical model of a distributed system with a path graph topology is shown in Fig. 2 and described as

$$X_n(s) = A_n(s) + B_n(s), \tag{8}$$

$$A_{n+1}(s) = G_+(s)A_n(s), \tag{9}$$

$$B_n(s) = G_-(s)B_{n+1}(s), \tag{10}$$

where $n \in \langle 1, N-1\rangle$, $G_+(s)$ and $G_-(s)$ are *asymmetric wave transfer functions* (AWTFs), which describe how the wave propagates in the system in the forward, (9), and backward directions, (10), respectively. It holds.

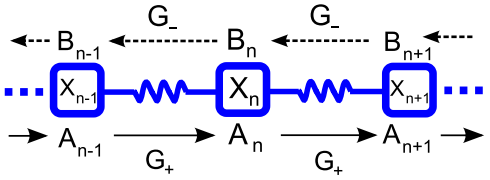

Fig. 2: Scheme of waves travelling in a distributed system with a path graph topology. The squares stand for agents and springs illustrate the virtual connections between the agents created by the controllers. Note that all the agents are identical.

Lemma 1. *AWTFs $G_+(s)$ and $G_-(s)$ are given by*

$$G_+(s) = \frac{1}{2}\beta(s) - \frac{1}{2}\sqrt{\beta^2(s) - 4\frac{M_\mathrm{f}(s)}{M_\mathrm{r}(s)}}, \tag{11}$$

$$G_-(s) = \frac{1}{2}\alpha(s) - \frac{1}{2}\sqrt{\alpha^2(s) - 4\frac{M_\mathrm{r}(s)}{M_\mathrm{f}(s)}}, \tag{12}$$

where

$$\alpha(s)=\frac{1+M_{\rm f}(s)+M_{\rm r}(s)}{M_{\rm f}(s)},\quad \beta(s)=\frac{1+M_{\rm f}(s)+M_{\rm r}(s)}{M_{\rm r}(s)}. \tag{13}$$

Proof: First, we find the transfer function describing the propagation in the forward direction, $G_+(s)$. The transfer function from $X_0(s)$ to $X_1(s)$ in a system with one leader and one follower is $X_1/X_0=M_{\rm f}/(1+M_{\rm f})$. For two followers is $X_1/X_0=(M_{\rm f}/M_{\rm r})\left(\beta-M_{\rm f}/(1+M_{\rm f})\right)^{-1}$. Continuing recursively for $N\to\infty$, X_1/X_0 is expressed by the continued fraction as

$$\frac{X_1(s)}{X_0(s)}=\cfrac{M_{\rm f}(s)/M_{\rm r}(s)}{\beta(s)-\cfrac{M_{\rm f}(s)/M_{\rm r}(s)}{\beta(s)-\ddots}} \tag{14}$$

Representing a square root function as the continued fraction, see [14],

$$\sqrt{z^2+y}=z+\cfrac{y}{2z+\cfrac{y}{2z+\ddots}}, \tag{15}$$

we have

$$\frac{X_1(s)}{X_0(s)}=\frac{1}{2}\beta(s)-\frac{1}{2}\sqrt{\beta^2(s)-4\frac{M_{\rm f}(s)}{M_{\rm r}(s)}}. \tag{16}$$

Similarly, we can find that

$$\frac{X_n(s)}{X_{n-1}(s)}=\frac{1}{2}\beta(s)-\frac{1}{2}\sqrt{\beta^2(s)-4\frac{M_{\rm f}(s)}{M_{\rm r}(s)}}. \tag{17}$$

The transfer function $G_-(s)$ describing the propagation in the opposite direction can be found analogously. Namely, let the leader be placed on the opposite end of the system. Then the transfer function from $X_0(s)$ to $X_{-1}(s)$ is

$$\begin{aligned}\frac{X_{-1}(s)}{X_0(s)}&=\cfrac{M_{\rm r}(s)/M_{\rm f}(s)}{\alpha(s)-\cfrac{M_{\rm r}(s)/M_{\rm f}(s)}{\alpha(s)-\ddots}}\\&=\frac{1}{2}\alpha(s)-\frac{1}{2}\sqrt{\alpha^2(s)-4\frac{M_{\rm r}(s)}{M_{\rm f}(s)}}.\end{aligned} \tag{18}$$

Note that the AWTFs can also be derived by the quadratic-equation approach given in Section 3.2 [12]. ∎

We note that the reflections of the wave from the leader and the rear-end agent described by the following Lemma are not used in the derivation of the main result of this paper. However, we feel obliged to derive them to fully cover the issue of waves in asymmetric bidirectional control. Moreover, we use the reflections for numerical verification of the proposed AWTF approach.

Lemma 2. *The reflections from the leader and the rear-end agent in the path graph are described by*

$$T_1(s)=\frac{A_1(s)}{B_1(s)}=-G_+(s)G_-(s), \tag{19}$$

$$T_N(s)=\frac{B_N(s)}{A_N(s)}=G_-(s)\frac{G_+(s)-1}{G_-(s)-1}, \tag{20}$$

respectively.

Proof: The position $X_1(s)$ in (3) can be rewritten as

$$X_1=\frac{1}{\alpha}X_0+\frac{1}{\beta}X_2. \tag{21}$$

Substituting for $X_1=A_1+B_1$ and $X_2=G_+A_1+G_-^{-1}B_1$ from (9) and (10), it yields

$$\begin{aligned}A_1&=\frac{1}{\alpha}\frac{1}{1-\frac{1}{\beta}G_+}X_0+\frac{1}{\beta}\frac{G_-^{-1}-\beta}{1-\frac{1}{\beta}G_+}B_1\\&=G_+X_0-G_+G_-B_1=G_+X_0+T_1B_1,\end{aligned} \tag{22}$$

where

$$\begin{aligned}&\frac{1}{\alpha}\frac{1}{1-\frac{1}{\beta}G_+}=\frac{1}{\frac{1}{2}\alpha+\frac{M_{\rm r}}{2M_{\rm f}}\sqrt{\beta^2-4\frac{M_{\rm f}}{M_{\rm r}}}}\\&=\frac{\frac{1}{2}\alpha-\frac{M_{\rm r}}{2M_{\rm f}}\sqrt{\beta^2-4\frac{M_{\rm f}}{M_{\rm r}}}}{\frac{1}{4}\alpha^2-\frac{1}{4}\left(\alpha^2-4\frac{M_{\rm r}}{M_{\rm f}}\right)}\\&=\frac{M_{\rm f}}{M_{\rm r}}\left(\frac{1}{2}\alpha-\frac{M_{\rm r}}{2M_{\rm f}}\sqrt{\beta^2-4\frac{M_{\rm f}}{M_{\rm r}}}\right)=\frac{1}{2}\beta-\frac{1}{2}\sqrt{\beta^2-4\frac{M_{\rm f}}{M_{\rm r}}}.\end{aligned} \tag{23}$$

Similarly,

$$\begin{aligned}&\frac{1}{\beta}\frac{G_-^{-1}-\beta}{1-\frac{1}{\beta}G_+}=(G_-^{-1}-\beta)\frac{1}{\frac{1}{2}\beta+\frac{1}{2}\sqrt{\beta^2-4\frac{M_{\rm f}}{M_{\rm r}}}}\\&=(G_-^{-1}-\beta)\frac{M_{\rm r}}{M_{\rm f}}G_+=-G_+G_-.\end{aligned} \tag{24}$$

Now, we derive the reflection relation for the rear-end agent. Substituting (9), (10) and (8) into (4) gives

$$A_N+B_N=M_{\rm f}(G_+^{-1}A_N+G_-B_N-A_N-B_N). \tag{25}$$

By rearranging, it gives

$$B_N=\frac{1+M_{\rm f}-M_{\rm f}G_+^{-1}}{M_{\rm f}G_--M_{\rm f}-1}A_N=G_-\frac{G_+-1}{G_--1}A_N, \tag{26}$$

where we have used $M_{\rm f}G_+^{-1}=-M_{\rm r}G_++(M_{\rm r}+M_{\rm f}+1)$ and $M_{\rm f}G_-=-M_{\rm r}G_-^{-1}+(M_{\rm r}+M_{\rm f}+1)$. ∎

To be able to track the leader travelling at a constant velocity with the zero steady-state error we require two integrators to be present in the model of each agent. The DC gains of the AWTFs in this case are limited to one as the following Lemma describes.

Lemma 3. *If there is at least one integrator in $M_{\rm f}(s)$ and $M_{\rm r}(s)$, then the DC gains of the AWTFs are*

$$\lim_{s\to0}G_+(s)=\kappa,\quad \lim_{s\to0}G_-(s)=1,\qquad \text{if } 0<\kappa<1, \tag{27}$$

$$\lim_{s\to0}G_+(s)=1,\quad \lim_{s\to0}G_-(s)=1/\kappa,\quad \text{if } \kappa\geq1, \tag{28}$$

where

$$\kappa=\lim_{s\to0}\frac{M_{\rm f}(s)}{M_{\rm r}(s)}=\frac{n_{\rm f,0}}{n_{\rm r,0}}. \tag{29}$$

Proof: First, we prove the DC gain of G_+. Substituting from (13) into (11) gives

$$G_+ = \frac{1}{2}\left(1 + \frac{1}{M_\mathrm{r}} + \frac{M_\mathrm{f}}{M_\mathrm{r}} - \sqrt{\left(1 + \frac{1}{M_\mathrm{r}} + \frac{M_\mathrm{f}}{M_\mathrm{r}}\right)^2 - 4\frac{M_\mathrm{f}}{M_\mathrm{r}}}\right). \tag{30}$$

Since we assume at least one integrator in M_r, $\lim_{s\to 0} 1/M_\mathrm{r} = 0$. Then

$$\begin{aligned}\lim_{s\to 0} G_+(s) &= \frac{1}{2}\left(1 + \kappa - \sqrt{(1+\kappa)^2 - 4\kappa}\right) \\ &= \frac{1}{2}(1 + \kappa - |1 - \kappa|),\end{aligned} \tag{31}$$

which proves (27). The proof of the DC gain of G_- is similar. ■

Another important characteristics of the AWTFs are the asymptotic stability and the $\mathcal{H}_\infty$ norm.

Theorem 1. *If $M_\mathrm{f}(s)$ and $M_\mathrm{r}(s)$ are proper and have no CRHP (closed-right half plane) zeros and no CRHP poles, except of p poles in the origin and if the Nyquist plot of*

$$T_G(s) = (M_\mathrm{f}(s) - M_\mathrm{r}(s))^2 + 2M_\mathrm{f}(s) + 2M_\mathrm{r}(s) + 1 \tag{32}$$

does not intersect the non-positive real axis, then the AWTFs are asymptotically stable.

Proof: We base the proof on Theorem A.2 [15], which states: *A linear system is stable if and only if its transfer function $T(s)$ is analytic in the right-half plane and $||T||_\infty < \infty$, where $||T||_\infty = \sup_{Re(s)>0} |T(s)|$.*

First, we prove that $||G_+(s)||_\infty < \infty$. We rewrite $\beta(s)$ in (13) as

$$\beta(s) = 1 + \frac{s^p d_\mathrm{r}(s)}{n_\mathrm{r}(s)} + \frac{d_\mathrm{r}(s) n_\mathrm{f}(s)}{d_\mathrm{f}(s) n_\mathrm{r}(s)}, \tag{33}$$

then $\lim_{s\to 0}\beta(s) < \infty$. Moreover, we assume that there are neither CRHP poles, nor CRHP zeros in $M_\mathrm{f}(s)$ and $M_\mathrm{r}(s)$, except of the p integrators. Therefore, the norm of $G_+(s)$ can be unbounded only for $s \to \infty$. The inverse of $G_+(s)$ is given by

$$G_+^{-1}(s) = \frac{1}{G_+(s)} = \frac{M_\mathrm{r}}{2M_\mathrm{f}}\left(\beta + \sqrt{\beta^2 - 4\frac{M_\mathrm{f}}{M_\mathrm{r}}}\right). \tag{34}$$

We denote m_β and m_r as the difference between the degrees of the numerator and the denominator in β and $M_\mathrm{r}/M_\mathrm{f}$, respectively. We can see from (33) that if M_r is proper, then: i) $m_\beta > 0$, ii) $(m_\beta + m_\mathrm{r}) \geq 0$, and iii) $\lim_{s\to\infty}\sqrt{\beta^2 - 4M_\mathrm{f}/M_\mathrm{r}} = \lim_{s\to\infty}\beta$. Therefore,

$$\lim_{s\to\infty} G_+^{-1} = \mu_\mathrm{m} s^{(m_\beta + m_\mathrm{r})} > 0, \tag{35}$$

where μ_m is a non-zero constant, and $\lim_{s\to\infty} G_+ < \infty$. Hence, $||G_+(s)||_\infty < \infty$. The proof of $||G_-(s)||_\infty < \infty$ is similar.

Next, we use the result of the complex function analysis, which states that the square root function $f(z) = \sqrt{z}$ is analytic everywhere except for the non-positive real axis (e.g., [16]). The square root function of $G_+(s)$ is

$$f_{2,+}(s) = \frac{1}{2}\sqrt{\beta^2(s) - 4\frac{M_\mathrm{f}(s)}{M_\mathrm{r}(s)}} = \frac{1}{2}\sqrt{\frac{1 + M_\mathrm{s}(s)}{M_\mathrm{r}^2(s)}}, \tag{36}$$

where $M_\mathrm{s} = M_\mathrm{r}^2 + M_\mathrm{f}^2 + 2M_\mathrm{r} + 2M_\mathrm{f} - 2M_\mathrm{r}M_\mathrm{f} = (M_\mathrm{r} - M_\mathrm{f})^2 + 2(M_\mathrm{r} + M_\mathrm{f})$. The overlapping branch cuts of $\sqrt{1/M_\mathrm{r}^2}$ cancel each other, therefore, $f_{2,+}$ is analytic if and only if $\sqrt{1 + M_\mathrm{s}}$ is analytic. Hence, if the Nyquist plot of $1 + M_\mathrm{s}$ does not intersect the non-positive real axis, then $f_{2,+}$ is analytic.

The first part of the AWTFs, $\alpha/2$ and $\beta/2$, are rational transfer functions. A rational function is analytic in the ORHP (open-right half plane) if and only if it has no singularities, in this case ORHP zeros and ORHP poles of M_f and M_r. Therefore, if M_f and M_r have no ORHP zeros, nor ORHP poles, then $\alpha/2$ and $\beta/2$ are analytic.

Since the difference of two analytic functions is also analytic, then both AWTFs are analytic. Both AWTFs have bounded $\mathcal{H}_\infty$ norm, hence, both are asymptotically stable. ■

Theorem 2. *If the AWTFs are asymptotically stable, there are two integrators in $M_\mathrm{f}(s)$ and $M_\mathrm{r}(s)$, and*

$$n_{\mathrm{f},0} \neq n_{\mathrm{r},0}, \tag{37}$$

$$d_{\mathrm{f},0} = d_{\mathrm{r},0} = 1, \tag{38}$$

$$n_{\mathrm{f},0} > 0,\ n_{\mathrm{r},0} > 0, \tag{39}$$

then either $||G_+(s)||_\infty > 1$ or $||G_-(s)||_\infty > 1$.

Proof: First, we prove that $||G_+||_\infty > 1$ if $\kappa > 1$, where $\kappa \neq 1$ due to (37). By ω_0 we denote a frequency that is close to 0 and evaluate the real and imaginary parts of the individual transfer functions as

$$x_1 + \jmath y_1 = \frac{M_\mathrm{f}(\jmath\omega_0)}{M_\mathrm{r}(\jmath\omega_0)},\ \ x_2 + \jmath y_2 = \frac{1}{M_\mathrm{r}(\jmath\omega_0)}, \tag{40}$$

$x = x_1 + x_2$ and $y = y_1 + y_2$. The Taylor series of (40) evaluated at zero yield

$$x_1(\omega_0) = k_{x,1} - k_{x,2}\omega_0^2 + k_{x,3}\omega_0^4 - ..., \tag{41}$$

$$y_1(\omega_0) = k_{y,1}\omega_0 - k_{y,2}\omega_0^3 + k_{y,3}\omega_0^5 - ..., \tag{42}$$

$$x_2(\omega_0) = -l_{x,1}\omega_0^2 + l_{x,2}\omega_0^4 - l_{x,3}\omega_0^6 + ..., \tag{43}$$

$$y_2(\omega_0) = -l_{y,1}\omega_0^3 + l_{y,2}\omega_0^5 - l_{y,3}\omega_0^7 + ..., \tag{44}$$

where we assumed that M_r has two integrators. We note that $k_{x,1} = \kappa$ and $l_{x,1} = 1/n_{\mathrm{r},0}$. The other coefficients, $k_{x,2}$, $k_{x,3}$, etc., obtained from Taylor series are not important due to limit $\omega_0 \to 0$ as we show later in the proof.

Substituting (40) into (11) gives the real part of $G_+(\jmath\omega_0)$ as

$$\mathrm{Re}\{G_+(\jmath\omega_0)\} = \frac{1}{2}(1 + x) - \frac{1}{2}\sqrt{\frac{|z| + \mathrm{Re}\{z\}}{2}}, \tag{45}$$

where we used $\mathrm{Re}\{\sqrt{z}\} = \sqrt{|z|/2 + \mathrm{Re}\{z\}/2}$, see e.g. Section 3.7.27 in [17], and

$$\begin{aligned} z &= \beta^2(\jmath\omega_0) - 4\frac{M_\mathrm{f}(\jmath\omega_0)}{M_\mathrm{r}(\jmath\omega_0)} \\ &= (1 + x^2 - y^2 + 2x - 4x_1) + \jmath(2y + 2xy - 4y_1). \end{aligned} \tag{46}$$

Next, we investigate the case when $\mathrm{Re}\{G_+(\jmath\omega_0)\} > 1$, hence, we solve the following inequality

$$(1+x) - \sqrt{\frac{|z| + \mathrm{Re}\{z\}}{2}} > 2. \tag{47}$$

We simplify it as

$$\big(2(x-1)^2 - \mathrm{Re}\{z\}\big)^2 - \mathrm{Re}\{z\}^2 - \mathrm{Im}\{z\}^2 > 0, \tag{48}$$

substitute into it from (46) and obtain

$$\begin{aligned} &- x_2(x_1-1)^2 - y_1y_2(x_1+x_2-1) - 2x_2^2(x_1-1) \\ &- x_2^3 - y_2^2(x_1+x_2) > 0. \end{aligned} \tag{49}$$

We substitute from (41)-(44) into (49) and get

$$l_{x,1}(k_{x,1}-1)^2\omega_0^2 + \mathcal{O}(\omega_0^4, \omega_0^6, \omega_0^8, ...) > 0, \tag{50}$$

where $\mathcal{O}(\omega_0^4, \omega_0^6, \omega_0^8, ...)$ stands for the polynomial with terms ω_0^4, ω_0^6, ω_0^8 etc. The lowest order term in (50) is ω_0^2. Therefore, the inequality in (47) holds for ω_0 close to zero if $l_{x,1} = 1/n_{\mathrm{r},0} > 0$. We assume in (39) that $n_{\mathrm{r},0} > 0$, hence, $\mathrm{Re}\{G_+(\jmath\omega_0)\} > 1$ and $||G_+||_\infty > 1$. Similarly, it can be shown that $||G_-||_\infty > 1$ if $0 < \kappa < 1$ and $n_{\mathrm{f},0} > 0$. Hence, if $n_{\mathrm{f},0} \neq n_{\mathrm{r},0}$ then $\kappa \neq 1$ and either $||G_+(s)||_\infty > 1$ or $||G_-(s)||_\infty > 1$ ■

IV. Implications for the graphs with asymmetric coupling

In this section, we follow the argument given in the Introduction that certain features in the performance of the distributed system can be inferred from the analysis of wave propagation between the agents because of the local nature of the AWTFs.

Definition 2. We say that the distributed system is *locally-string stable* if the AWTFs are asymptotically stable and

$$||G_+(s)||_\infty \leq 1 \quad \text{and} \quad ||G_-(s)||_\infty \leq 1. \tag{51}$$

Otherwise, the system is called *locally-string unstable*.

The meaning of the local-string stability is similar to the string stability. Both the local-string stability and the string stability deal with the performance of the distributed system and describe whether the disturbance acting on an agent amplifies as it propagates through the system. However, the local-string stability describes the performance from the local point of view without considering the whole distributed system. The local description is particularly advantageous for a large distributed system, where the traditional Laplacian approach is difficult to apply.

The main contribution of the paper is given in the following Theorem.

Theorem 3. *If i) all agents are identical, ii) there are two integrators in the dynamics of the agents, and iii) the positional coupling between the agents is asymmetric, then the distributed system is locally-string unstable.*

Proof: If the positional coupling is asymmetric, then $n_{\mathrm{f},0}/d_{\mathrm{f},0} \neq n_{\mathrm{r},0}/d_{\mathrm{r},0}$ by Definition 1. Since we can always transform $M_{\mathrm{f}}(s)$ and $M_{\mathrm{r}}(s)$ such that $d_{\mathrm{f},0} = d_{\mathrm{r},0} = 1$, then $n_{\mathrm{f},0} \neq n_{\mathrm{r},0}$. Therefore, $||G_+(s)||_\infty > 1$ or $||G_-(s)||_\infty > 1$, which follows from Theorem 2, and the distributed system is locally-string unstable. ■

We can interpret Theorem 3 as follows. The $||G_+(s)||_\infty > 1$ causes that the disturbance is amplified as it propagates from $X_i(s)$ to $X_{i+1}(s)$, from $X_{i+1}(s)$ to $X_{i+2}(s)$, from $X_{i+2}(s)$ to $X_{i+3}(s)$ etc. The larger the path graph is, the more is the disturbance amplified. Similarly, if $||G_-(s)||_\infty > 1$, then the disturbance is amplified as it propagates in the opposite direction.

Theorem 3 is in agreement with the results of [9], [4] or [10], which state that if the asymmetry is in the form of $M_{\mathrm{f}}(s) = \mu M_{\mathrm{r}}(s)$ with μ being a constant gain, then the system is string unstable. However, Theorem 3 is more general since it states that the distributed system is string unstable if the DC gain of $M_{\mathrm{f}}/M_{\mathrm{r}}$ is not equal to one. Hence, it allows the asymmetry to be more complex.

We should emphasize that Theorem 3 does not disprove an asymmetry in the velocity coupling. In fact, the asymmetric velocity coupling may improve the transient of the system, as shows the simulation example in Section V.

V. Mathematical simulations

The mathematical simulations compare three different control strategies for two different sizes of a path graph. The results are shown in Fig. 3, where the agent is modelled as a double integrator with a linear model of friction controlled by a PI controller, that is

$$M_{\mathrm{f}} = \frac{1}{3}\frac{4s+4}{s^2(s/3+1)} \tag{52}$$

for all three cases. But

$$M_{\mathrm{r}} = M_{\mathrm{f}}, \quad M_{\mathrm{r}} = \frac{2.5}{4}M_{\mathrm{f}}, \quad M_{\mathrm{r}} = \frac{1}{3}\frac{2.5s+4}{s^2(s/3+1)}, \tag{53 a, b, c}$$

for the left, middle and right panels, respectively.

We can see that the symmetric bidirectional control has a very long transient (the left panel), which is shortened when the asymmetry is introduced to both positional and velocity couplings (the middle panel). However, the asymmetry in the positional coupling causes a large overshoot which even scales with the size of the graph. When the positional coupling is kept symmetric and the velocity coupling asymmetric (the right panel), the overshoot is smaller than for the symmetric case. Moreover, we can see that the transient scales approximately linearly with the size of the graph.

An independent validation of the AWTF approach is shown in Fig. 4. We can see excellent agreement between the state-space approach based on (3) and the AWTF approach.

Fig. 5 shows the numerical validation of Theorem 2 for M_{f} and M_{r} defined by (52) and (53b)-(53c). We can see that, if there is asymmetry in the positional coupling (solid line), i.e. $n_{\mathrm{f},0} \neq n_{\mathrm{r},0}$, then the $\mathcal{H}_\infty$ norm of G_+ is greater than one. The norm is reduced to one by making the positional coupling symmetric (dashed line).

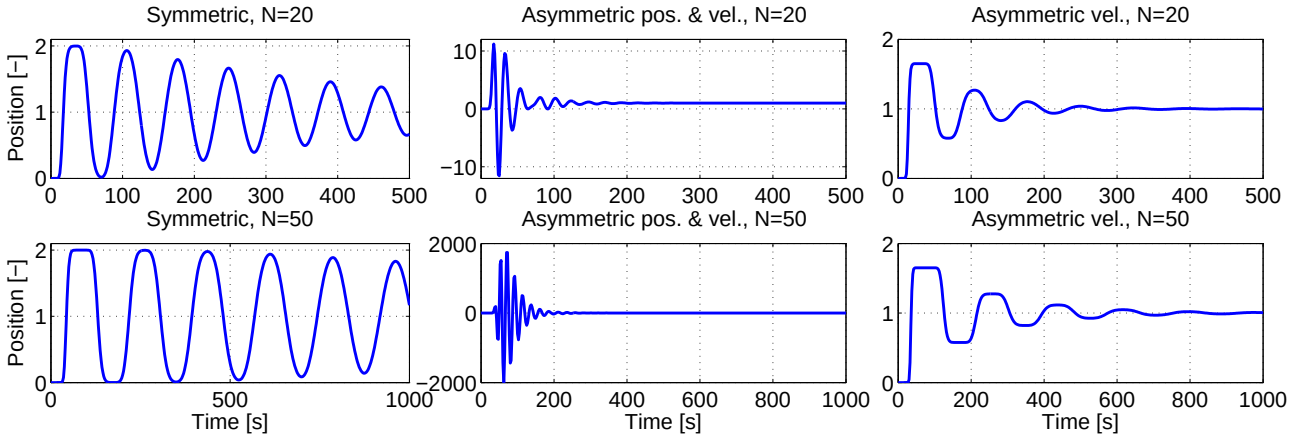

Fig. 3: The numerical simulations showing the position of the last agent in the distributed system with path graph topology when the leader changes its position from 0 to 1. The figure compares three different bidirectional control strategies: i) the symmetric (the left panels) defined by (53a), ii) the traditional asymmetric control with asymmetries in both positional and velocity couplings (the middle panels), see (53b), and iii) the combined symmetric positional with asymmetric velocity couplings (the right panels), see (53c). The top and bottom panels show the system with 20 and 50 agents, respectively.

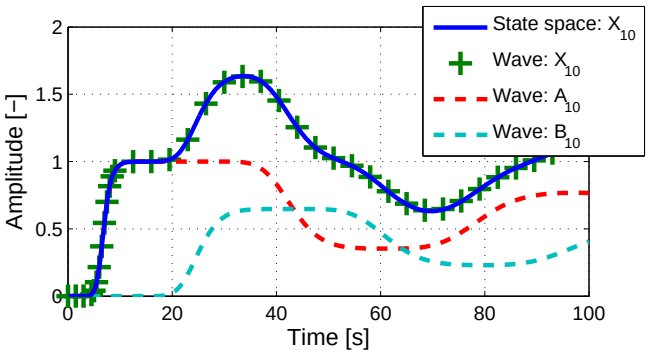

Fig. 4: The comparison of the positions of the 10th agent in the system considered at the top right panel in Fig. 3 simulated by the state-space approach using (3) (blue solid line) and by the AWTF's approach using (9), (10) and Lemmas 1 and 2 (green crosses). The two components A_{10} and B_{10} from (8) are shown with the dashed red and blue lines, respectively.

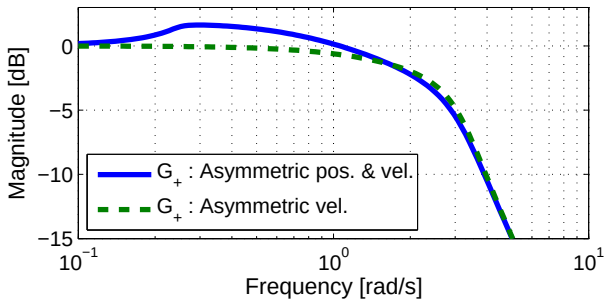

Fig. 5: The comparison of the frequency characteristics for two different transfer functions $G_+(s)$. The asymmetries in the couplings are defined as in Fig. 3.

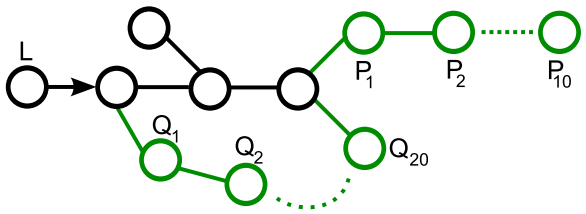

Fig. 6: The topology of the distributed system, where the black and green nodes represent the agents with the symmetric and asymmetric couplings, respectively. The 'L'-node is the leader of the system. 'Q'-nodes lie on the same path, which differs from the path of 'P'-nodes.

VI. Relation to systems with other graph topologies

The numerical simulations in the previous section are carried out for a distributed system with a path graph topology. However, Theorem 3 holds also for a more complex graphs because of the local nature of the AWTFs. This can be nicely demonstrated on a graph, where a path graph is a part of a more complex graph as in Fig. 6. Although, the string stability is defined and studied mostly for the path graphs, we can observe the same phenomenon, that is, the amplification of a disturbance as it propagates in the system. The top panels of Fig. 7 show that the condition of the symmetric positional coupling is violated. Such a phenomenon is difficult to identify by the traditional state-space approach.

VII. Conclusions

The paper examined a distributed system with asymmetric bidirectional control, where the coupling between the agents is allowed to be arbitrarily complex. The proposed approach reveals that the symmetric positional coupling, i.e. identical DC gains of the controllers, is necessary for the string stability of the distributed system. This finding does not disprove the asymmetry for other couplings. In fact, it is numerically shown

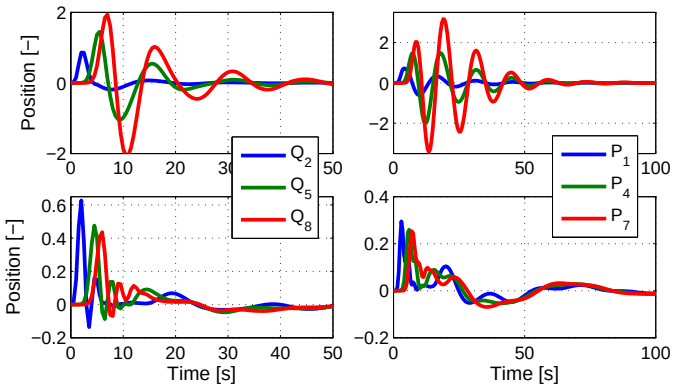

Fig. 7: The numerical simulations showing the positions of agents Q_2, Q_5, Q_8, P_1, P_4 and P_7 of the system with the topology in Fig. 6. The input to the system is the Dirac pulse, which represents the noise acting on the leader. The agents at the top and bottom panels have M_{f} and M_{r} defined as in middle and right panels in Fig. 3, respectively.

that, if the asymmetry in the velocity coupling is adjusted properly, then the system's performance may be improved.

REFERENCES

[1] J. Eyre, D. Yanakiev, and I. Kanellakopoulos, "A Simplified Framework for String Stability Analysis of Automated Vehicles∗," *Vehicle System Dynamics*, pp. 375–405, 1998.

[2] J. Ploeg, N. van de Wouw, and H. Nijmeijer, "Lp String Stability of Cascaded Systems: Application to Vehicle Platooning," *IEEE Transactions on Control Systems Technology*, vol. 22, no. 2, pp. 786–793, Mar. 2014.

[3] D. Swaroop and J. Hedrick, "String stability of interconnected systems," *IEEE Transactions on Automatic Control*, vol. 41, no. 3, pp. 349–357, Mar. 1996.

[4] F. Tangerman, J. Veerman, and B. Stosic, "Asymmetric decentralized flocks," *IEEE Transactions on Automatic Control*, vol. 57, no. 11, pp. 2844–2853, 2012.

[5] C. E. Cantos and J. J. P. Veerman, "Transients in the Synchronization of Oscillator Networks," *eprint arXiv:1308.4919*, 2014.

[6] B. Bamieh, M. R. Jovanovic, P. Mitra, and S. Patterson, "Coherence in Large-Scale Networks: Dimension-Dependent Limitations of Local Feedback," *IEEE Transactions on Automatic Control*, vol. 57, no. 9, pp. 2235–2249, Sep. 2012.

[7] P. Seiler, A. Pant, and K. Hedrick, "Disturbance Propagation in Vehicle Strings," *IEEE Transactions on Automatic Control*, vol. 49, no. 10, pp. 1835–1841, Oct. 2004.

[8] H. Hao and P. Barooah, "On Achieving Size-Independent Stability Margin of Vehicular Lattice Formations With Distributed Control," *IEEE Transactions on Automatic Control*, vol. 57, no. 10, pp. 2688–2694, Oct. 2012.

[9] P. Barooah, P. Mehta, and J. Hespanha, "Mistuning-Based Control Design to Improve Closed-Loop Stability Margin of Vehicular Platoons," *IEEE Transactions on Automatic Control*, vol. 54, no. 9, pp. 2100–2113, Sep. 2009.

[10] I. Herman, D. Martinec, Z. Hurak, and M. Sebek, "Nonzero bound on Fiedler eigenvalue causes exponential growth of H-infinity norm of vehicular platoon," *IEEE Transactions on Automatic Control*, vol. 9286, no. c, pp. 1–1, 2014.

[11] H. Hao, H. Yin, and Z. Kan, "On the robustness of large 1-D network of double integrator agents," in *American Control Conference (ACC)*, 2012, pp. 6059–6064.

[12] D. Martinec, I. Herman, Z. Hurák, and M. Šebek, "Wave-absorbing vehicular platoon controller," *European Journal of Control*, vol. 20, pp. 237–248, 2014.

[13] R. Olfati-Saber, J. Fax, and R. Murray, "Consensus and cooperation in networked multi-agent systems," *Proceedings of the IEEE*, no. January, pp. 215–233, 2007.

[14] W. B. Jones and W. J. Thron, *Continued Fractions: Analytic Theory and Applications*, ser. Encyclopedia of Mathematics and its Applications. New York: Cambridge University Press, 1984.

[15] R. Curtain and K. Morris, "Transfer functions of distributed parameter systems: A tutorial," *Automatica*, vol. 45, no. 5, pp. 1101–1116, May 2009.

[16] E. M. Stein and R. Shakarchi, *Complex Analysis*, ser. Princeton lectures in analysis. New Jersey: Princeton University Press, 2010.

[17] M. Abramowitz and I. Stegun, *Handbook of mathematical functions: with formulas, graphs, and mathematical tables*. Dover Publications, 1964.